Novel anticorrosive zinc phosphate coating for corrosion prevention of reinforced concrete

Ahmed Elshami, Stéphanie Bonnet, Abdelhafid Khelidj, Latefa Sail

▶ **To cite this version:**

Ahmed Elshami, Stéphanie Bonnet, Abdelhafid Khelidj, Latefa Sail. Novel anticorrosive zinc phosphate coating for corrosion prevention of reinforced concrete. European Journal of Environmental and Civil Engineering, 2016, 21 (5), pp.572-593. 10.1080/19648189.2016.1139507 . hal-01398608

HAL Id: hal-01398608
https://hal.science/hal-01398608

Submitted on 1 Feb 2024

HAL is a multi-disciplinary open access archive for the deposit and dissemination of scientific research documents, whether they are published or not. The documents may come from teaching and research institutions in France or abroad, or from public or private research centers.

L'archive ouverte pluridisciplinaire **HAL**, est destinée au dépôt et à la diffusion de documents scientifiques de niveau recherche, publiés ou non, émanant des établissements d'enseignement et de recherche français ou étrangers, des laboratoires publics ou privés.

Novel anticorrosive zinc phosphate coating for corrosion prevention of reinforced concrete

Ahmed A. Elshami[a]*, Stéphanie Bonnet[b], Abdelhafid Khelidj[b] and Latefa Sail[c]

[a]*Housing & Building National Research Centre (HBRC), Dokki, Giza, Egypt;* [b]*Institute Research of Civil Engineering and Mechanical, LUNAM University, University of Nantes – IUT of Saint-Nazaire, GeM, CNRS UMR 6183, France;* [c]*EOLE Laboratory, Civil Engineering Department, Abou Bakr Belkaid University, PB 230, Chetouane, Tlemcen, Algeria*

Deterioration of reinforcing concrete structures is a common problem among all the coast countries. Every year, several billion dollars are spent to repair and maintain reinforced concrete structures. Over time, the metal reinforcing bars used to improve the properties of concrete become susceptible to corrosion due to factors such as the presence of chloride and carbonation. Present work includes the use of novel anticor-rosive coating. The use of zinc phosphate (ZP) coating has advantage of the low sol-ubility of phosphates in medium- or high-pH solutions; also the resulting coating remains adhered to the metal surface even under extreme deformation. This study presents the efficiency of a new inhibitive pigment ZP containing zirconium com-pound obtained by chemical conversion (CC) method and cathodic protection to pro-tect the steel rebars against localised corrosion in concrete. The corrosion behaviour of coated steel was assessed by open circuit potential, potentiodynamic polarisation and electrochemical impedance spectroscopy. Firstly, results demonstrated that the new coating show an adsorption on steel surface and provides an effective corrosion resistance compared to carbon steel rebar. Secondly, results showed that the increased weight of coating made by CC is consistent with the development of the polarisation resistance and corrosion potential of samples studied. Thirdly, a reduction in the corrosion rate is obtained once the coating covers the surface of the metal.

Keywords: concrete; corrosion; chloride; carbon steel; zinc phosphate

1. Introduction and scientific background

This study completes the work of the researchers (Burokas and semescu) on zinc phosphate (ZP) coating and develops it. We use the same compositions of those researchers but change the concentration of those compositions. According to the previous literature, (Burokas, Martušienė, & Bikulčius, 1998) reported that ZP coatings occurred on separate sites and did not cover the entire surface in the presence of chloride.

However, (Simescu, 2008) showed that if the time required for initiation of corrosion in steel coated by ZP increased more than uncoated steel, then depassivation occurred. (Manna, 2009; Zeng, Lan, Kong, Huang, & Cui, 2011) If the diameter of coated steel increased, then corrosion onset delayed.

Many researchers are inclined to use well-controlled synthetic solutions to emulate concrete environment (Nedal, 2009). Most of the existing research generally agrees that

*Corresponding author. Email: materialhnbrc@yahoo.com

the Cl^-/OH^- threshold ratio for carbon steel in synthetic solutions is < 1 (Alonso, Andrade, Castellote, & Castro, 2000; Hurley, 2007). We study the efficiency of ZP coating in synthetic pore solutions with and without chloride.

In the previous literature, zinc oxide with phosphoric acid has been studied as phosphate coatings (González, Ramírez, & Bautista, 1998; Veleva, Alpuche-Aviles, Graves-Brook, & Wipf, 2005). Significant variations in the morphology, adhesion and corrosion protection observed with the Cu^{2+} in the bath, zirconium and Ni^{+2} ions are used for their active role in the germination and growth of phosphate crystals (Kouisni, Azzi, Zertoubi, Dalard, & Maximovitch, 2004; Zimmermann, Mun˜oz, & Schultze, 2005).

Firstly, we study the effectiveness of different coatings of ZP formed by chemical conversion (CC) on corrosion prevention of reinforced concrete: the best coating will be selected. Secondly, the selected coatings will be formed by cathodic electrochemical treatment (CET) on reinforcing bars to study their stability and efficiency in solutions emulating concrete. These tests, in simulated concrete pore solutions, are necessary to understand the protection ability of ZP coatings, prior to their application on reinforcing bars embedded in concrete.

2. Experimental study

The experimental study includes three steps. The first two steps are led to choose the best coating product by testing referencing bars in simulating solution. The last one is about the efficiency of this coating when reinforcing bars are embedded in concrete.

In the first step, thirty baths of ZP were developed and formed by CC.

- 10 baths with different concentration of nitric acid;
- 10 baths with different concentration of nickel sulphate;
- 4 baths with different concentration of copper and zirconium;
- 6 baths with different concentration of phosphoric acid.

The compositions of the different baths are similar to that used by Simescu, 2008; Adhikari et al., 2011; Andreatta et al., 2011; Simescu & Idrissi, 2009).

The efficiency was evaluated by electrochemical measurements and scanning electron microscope (SEM) and energy dispersive spectroscopy (EDS) analysis: we chose the best three baths according to the highest three values of polarization resistance from each type of bath.

In the second step, the best three baths are used by CET to study steel corrosion in pore solution. In the third step, we use the high-quality bath from the best three baths to study steel corrosion in Portland cement mortar. Six steel (repeatability for one test) placed in pore solutions more or less corrosive and simulating more or less degraded concrete was investigated through electrochemical methods (Figure 1).

2.1. Chemical conversion

Metallic coatings are obtained either by galvanisation (for zinc) or by conversion (phosphating and chromating). Conversion coatings are also known as chemical treatments. On this basis and also for economic reasons, we chose the phosphate CC to improve the corrosion resistance of steel in concrete.

The first method of our experimental work focused on the development and achievement of the phosphate coating by CC. The conversion coating is a coating for metals

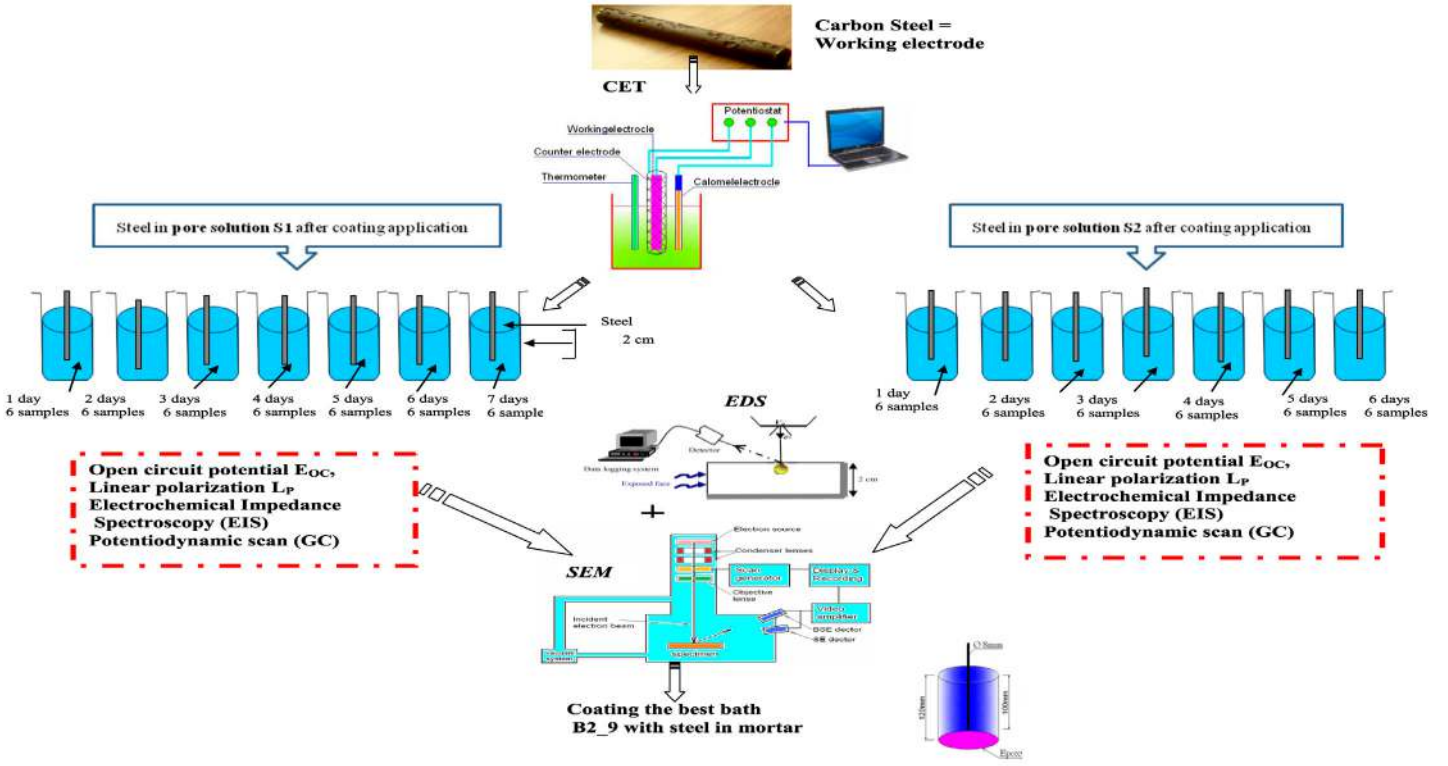

Figure 1. Experimental steps of influence of zinc phosphate coating on steel protection by CET.

where the part surface is converted into the coating with a chemical process. This chemical process has some advantages such as quality improvement in high temperature, manufacturing technology simple to install and no toxic (Simescu, 2008). The tests of CC are including variation in concentration of the different components and modifications in the composition of ZP coating.

2.1.1. *Cell treatment and polarisation resistance* R_P

The cell is a straight-sided glass jar that had a wide mouth covered with a plastic cap with three holes to fit the two electrodes and thermometer.

The CC was performed on six steel at 60 °C.

Experiments were conducted using carbon steel bars with a diameter of 8 mm which is called working electrode. Saturated calomel electrode (SCE) (reference electrode) was used to measure the potential of the working electrode. Two sets of graphite electrodes which are called counter electrodes complete the electrical circuit.

Before being tested as per ASTM [G1-03], the working electrodes were cleaned by a pickling solution for the removal of unwanted deposits or rust over the surface of the rods. Carbon steel samples were dipped in a pickling solution which consists of 184 millilitres of hydrochloric acid (37%), 2 g hexamethylene tetramine and the balance deionised water to make 1 l of solution. After cleaning, the bars were rinsed, dried with hot forced-air and weighed to the nearest 0.0001 g. Finally, the cleaned bars were photographed and stored in dessicators to prevent further atmospheric corrosion. During this treatment, vinyl examination gloves were worn to prevent contamination.

CC treatment was performed in the phosphating bath (pH < 3) for 10 min at 60 °C. The phosphated surface (steel surface immersed in the phosphating bath) was approximately a cylinder with a length of 2 cm corresponding to a surface area of 5.02 cm^2. The operating conditions, temperature and time treatment, are determined to obtain a well-crystalline coating (Simescu, 2008).

The chemical compositions of the metals under investigation and the parameters used in corrosion rate calculations for the metals under investigation are shown in Table 1.

The density of the metal tested is 7870 kg/m^3. The equivalent weight is the theoretical mass of metal that will be lost from the sample after one Faraday of anodic charge has been passed (0.02792 kg/eq.). These parameters are used in corrosion rate calculations.

This study intended to investigate the electrochemical behaviour:(extrapolation of the linear polarisation resistance R_P was made with the help of EC-Lab software during the treatment (10 min)(Simescu, 2008).

2.1.2. *SEM and EDS analysis*

With a sample of steel treatment with flat section and coupled detectors on either side of the beam, topographic contrast is effectively eliminated. After treatment, the

Table 1. Chemical composition of carbon steel for concrete reinforcement.

Metal	C (%) Max	Mn (%) Max	Si (%) Max	N(%) Max	S (%) Max	P(%) Max	CEV (%) Max
Carbon steel	0.22	0.58	0.18	0.013	0.05	0.05	0.52

microstructure of surface of steel is evaluated by means of scanning electron microscope (SEM) using an environmental Zweiss EVO®40 system. Two-dimensional images of samples at different ages are attained. The schematic representation of the microscope was used in this work to estimate the particle shapes and to determine the elements deposited on steel surface to estimate the formation of film pigments. Energy-dispersive X-ray spectroscopy (EDS) is to identify and measure the mass percentage of each element perpendicular only on steel surface treated by ZP coating.

2.2. Cathodic electrochemical treatment (CET)

CET was applied only with three best baths selected after CC treatment. This electrochemical process has some advantages such as it does not require specific addition, has good quality at low temperature, has stable coating in NaCl solution, is suitable for localised protection and is economic (Simescu, 2008). Also, this electrochemical process is 10 min for both CC and CET.

After CET, the steel was immersed in solutions simulating pore concrete solution with and without chloride to evaluate the efficiency of coatings by electrochemical measurement.

2.2.1. Cell treatment

The corrosion cell used for CET and corrosion measurement is almost the same that is used with CC except titanium/platinum which is used as counter electrode and thermostat to measure the temperature.

The treatment was used on six steel to facilitate process treatment and with and without chloride without disturbing the sample.

CET is performed at an applied potential of −1800 mV vs. SCE, for 10 min at room temperature. During testing, the three electrodes were attached to a Biologic Ec-Lab potentiostat instrument. The aim of this method was to produce a potential imposed or a density imposed current in order to obtain a larger thickness at the room temperature and at shorter treatment times (<10 min).

2.2.2. Corrosion within pore solution (S1 & S2) and electrochemical measurements

Firstly, a saturated calcium hydroxide solution (noted S1) has been used to simulate the aqueous alkaline content of the (non-carbonated) concrete pore solution, with an approximate pH of 13 (Simescu, 2008). Secondly, to simulate the aqueous phase of a concrete contaminated with chloride, an electrolyte designated by S2 was used. This one contains $Ca(OH)_2$ saturated solution and 3.5% NaCl. This chloride content is higher than critical threshold by approximately 20 times. The initial pH measured was 13, but it dropped to a value of 12.5 ± 0.05 due to the chloride addition and possible carbonation from air during pouring into the corrosion cells (Nedal, 2009) (Table 2).

Table 2. Description of the various electrolytes used.

Solution	$Ca(OH)_2$ (mol/L)	NaOH (mol/L)	KOH (mol/L)	NaCl (g/L)	KCl (mol/L)	PH
S1	Saturation	0.001	0.001	0	0.0	12.7
S2	Saturation	0.001	0.001	35	0.006	12.5

In this study, we investigate the electrochemical behaviour of carbon steel with coating in both solutions. This investigation is carried out using direct current DC measurements techniques (open circuit potential E_{OC}, linear polarisation L_P and potentiodynamic scan GC). The electrochemical impedance spectroscopy (EIS) technique was used to investigate the change in the electrochemical properties of the passive film formed on the metal surface when steel is immersed in S1 and S2.

2.2.3. SEM and EDS analysis

The same procedure as described in 2.1.2 was used on steel.

2.3. Steel samples embedded in mortar

The best bath was selected after analysing results obtained after CET and immersion in S1 and S2. The last step is to test this coating in the case of steel embedded in OPC mortar. In order to measure the corrosion currents in a concrete environment, a set of six carbon steel rebar samples embedded in OPC mortars pre-contaminated with NaCl at 5% of cement weight were prepared. The chemical compositions of Portland cement CEM I and mortar composition are given in Table 3. The NaCl was dissolved in the mixing water before being added to the mortar mix. The amount of NaCl 5% per cement weight was chosen to guarantee rebar corrosion initiation and corrosion currents inside mortar (Nedal, 2009).These rebars were treated by CET with the best coating selected after step 2. After mixing water, cement and sand, the mortar produced was poured into cylinder of 110 mm diameter and 120 mm length in which carbon steel was placed according to its longitudinal axis. The samples were compacted and were removed from the moulding after one day. After the demoulding, the samples were

Table 3. Chemical compositions of OPC and mortar.

Compounds	% (By weight)	Composition of mortar	
	Cement	Component weight (kg/m^3)	OPC mortar
CaO	64.95	Portland cement CEM I	350
SiO_2	21.25	Slag	–
Al_2O_3	3.47	Water	168
Fe_2O_3	4.23	Normal sand	868
MgO	0.96	Water/cement	0.48
K_2O	0.28	NaCl	17.5
Na_2O	0.10	Mechanical properties for OPC concrete	
SO_3	2.63	90-day compressive strength	59
Specific surface (m^2/kg)	382		
Density (–)	3.18		
Main compounds (Bogue's equation) % by weight			
C_3S	67.5		
C_2S	10.7		
C_3A	2.64		
C_4AF	12.8		
Gypsum	3.3		

stored in moist at 20 ± 2° C and over 95 ± 5% of relative humidity for 90 days. To accelerate more the penetration of chlorides, slabs are only partially immersed. The saline solution used is composed by 35 $g.L^{-1}$ of salt is so nearly 20 $g.L^{-1}$ of chlorides. Then, an epoxy resin coating was applied to the lower face of the sample to ensure that the concrete pore penetrates only through the lateral surface in order to simulate a propagation of the chloride front in a single direction.

3. Results and discussion on ZP coating steel

3.1. Coatings obtained by CC method

The study, by Burokas et al., 1998, was the first application of light- to medium-weight non-metallic ZP coating to steel surfaces. ZP coating permits the distribution and retention of a uniform film over the entire surface and prevents metal-to-metal contact and extrusion of more difficult shapes than is possible without the coating. We chose Burokasbath (Zn^{2+}, Ni^{2+}, NO_3^-, PO_4^{3-}) as the reference, and we added different compounds ($NaNO_2$, NaC_6H_5COO, $Na_3C_6H_5O_7$) to develop characters of the coating (Table 4). These compounds are present and constant except $Na_3C_6H_5O_7$. Thirty baths were tested.

3.1.1. Baths based on sodium nitrite, benzoate and citrate under the influence of nitrate (NO_3^-) (Table 4)

These baths under the influence of nitric acid and the concentration of nitric acid decreased gradually from 11 ml/l in B1-1 until 1.5 ml/l in B1-9. Figure 2 illustrates the values of polarisation resistance of different baths up to 10 minutes of treatment. Each point of the polarisation resistance in the Figure 2 is obtained from six tests. The polarisation resistance of the coating formed on steel surface was increased during phosphating treatment due to the change in the concentration of nitric acid. When the concentration of nitric acid decreases, the coating thickness increases. At the same time, we noted that the pH of the phosphating solution increases with the decrease in nitric acid in the bath. The change in the concentration of nitric acid leads to a decrease in the kinetic treatment after 4 to 5 min and precipitation of the remaining ZP at the bottom of the bath, and this is noted by naked eye.

Table 4. Compositions of baths based on zinc oxide, nickel sulphate.

Bath number	Composition	pH
B1	Burokas et al., 1998 + $NaNO_2$(0.5 g/L), NaC_6H_5COO(0.5 g/L), $Na_3C_6H_5O_7$(20 g/L)	2.7
B1-1	BathB1 + HNO_3(11 ml/L)	1.4
B1-2	BathB1 + HNO_3(9.5 ml/L)	1.5
B1-3	BathB1 + HNO_3(8.0 ml/L)	1.7
B1-4	BathB1 + HNO_3(7.5 ml/L)	1.8
B1-5	BathB1 + HNO_3(6.5 ml/L)	1.9
B1-6	BathB1 + HNO_3(5.5 ml/L)	2.05
B1-7	BathB1 + HNO_3(4.5 ml /L)	2.2
B1-8	BathB1 + HNO_3(3.3 ml /L)	2.5
B1-9	BathB1 + HNO_3(1.5 ml /L)	2.6

Table 5. Compositions of baths based on citrate ions and hexametaphosphate.

Bath number	Composition	pH
B2	Burokas et al., 1998 + $NaNO_2$(0.5 g/L), $Na_6P_6O_{18}$ (2.5 g/L),NaC6H5COO (0.5 g/L), $Na_3C_6H_5O_7$(15 g/L)	2.7
B2-1	Bath2 + $NiSO_4$*$6H_2O$(23.9 g/L)	3.9
B2-2	Bath2 + $NiSO_4$*$6H_2O$(19.8 g/L)	3.7
B2-3	Bath2 + $NiSO_4$*$6H_2O$(17.6 g/L)	3.5
B2-4	Bath2 + $NiSO_4$*$6H_2O$(15.2 g/L)	3.3
B2-5	Bath 2 + $NiSO_4$*$6H_2O$(11.77 g/L)	3.1
B2-6	Bath 2 + $NiSO_4$*$6H_2O$(8.21 g/L)	3.0
B2-7	Bath2 + $NiSO_4$*$6H_2O$(5.3 g/L)	2.9
B2-8	Bath2 + $NiSO_4$*$6H_2O$(3.5 g/L)	2.8
B2-9	Bath2 + $NiSO_4$*$6H_2O$(1.27 g/L)	2.7

Table 6. Compositions of baths with various amounts of cupper and zirconyl.

Bath number	Composition	pH
B3	Burokas et al., 1998 + $NaNO_2$ (0.5 g/L), NaC_6H_5COO (0.5 g/L), $Na_3C_6H_5O_7$(10 g/L)	2.5
B3-1	Bath3 + ZrO $(NO_3)_2$. H_2O (0.0006 g/L), CuO(0.0006 g/L)	3.0
B3-2	Bath3 + ZrO $(NO_3)_2$. H_2O (0.0012 g/L), CuO(0.0012 g/L)	3.2
B3-3	Bath3 + ZrO $(NO_3)_2$. H_2O (0.0024 g/L), CuO(0.0024 g/L)	3.4

Table 7. Compositions of baths with various amounts of phosphorous.

Bath number	Composition	pH
B4	Burokas et al., 1998 + $NaNO_2$ (0.5 g/L), NaC6H5COO(0.5 g/L), $Na_3C_6H_5O_7$(5.0 g/L), $Na_6P_6O_{18}$ (1.5 g/L), (pH < 3)	2.1
B4-1	Bath4 + H_3PO_4(19.3 ml/L)	1.1
B4-2	Bath4 + H_3PO_4(17.15 ml/L)	1.3
B4-3	Bath4 + H_3PO_4(15.52 ml/L)	1.7
B4-4	Bath4 + H_3PO_4(12.83 ml/L)	1.8
B4-5	Bath4 + H_3PO_4(10 ml/L)	1.9

Results showed that the increased quality of coating made by (CC) is consistent with the development of the polarisation resistance. Figure 2 shows in the beginning of the phosphating process (50 s at 60 °C) that the polarisation resistances are, respectively, around 100–400 Ohm cm^2 for B1-1 and around 1000 Ohm cm^2 for B1-9. But after 5–10 min of phosphating process, the polarisation resistances increase from 1000 to 9000 Ohm cm^2 for (B1-9).For (B1-1), the polarisation resistance remains almost constant with increasing time ranging from 400 to 1000 Ohm cm^2 by the decrease in the concentration of nitric acid. For (B1-1 and B1-9), the polarisation resistance increased because of the decrease in acid content and presence of anions of nitrite. These reasons lead to increase the chance for the formation of phosphophyllite in the phosphate coating. This phosphophyllite increases the charge transfer resistance which controls the speed of metal dissolution into the electrolyte; therefore, it is more difficult to reach the conditions necessary to promote decrease in polarisation resistance.

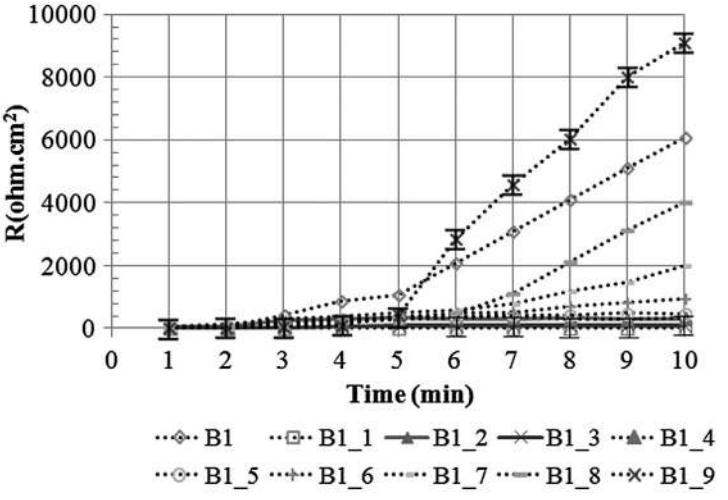

Figure 2. Values of polarisation resistance.

The acidity of the bath used has an influence on the formation of phosphate crystals on the surface of the steel.

Scanning electron microscope (SEM) values after 24 h (to enable coating film to cohere on surface of steel) of steel treatment are plotted in Figure 3. It shows a group of hopeite Zn_3 (PO_4) $4H_2O$ characterised by adjacent golf balls for B1_9 in comparison with B1_1 which occurred on separate sites and did not cover the entire surface.

The coating obtained from EDS analysis has 13% phosphorus, zinc 37.2% and amount of iron is 39.9% for B1_9 (Simescu, 2008).However, B1-1 has 7.5% phosphorus, 19% of zinc and 53,4% of iron.

3.1.2. Baths based on hexametaphosphate and citrate ions under the influence of nickel (Table 5)

We have prepared a bath from $Na_6P_6O_{18}$ to decrease the surface roughness and increase the absorption of ZP compounds and added various amount of nickel sulphate from 23.9 g/l to 1.27 g/l.

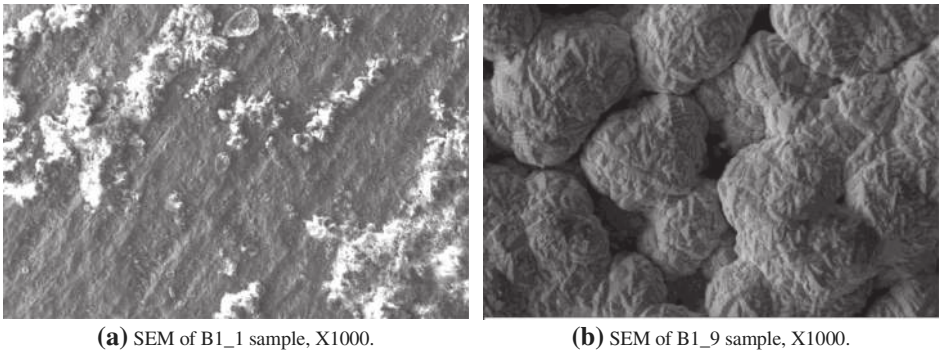

(a) SEM of B1_1 sample, X1000. **(b)** SEM of B1_9 sample, X1000.

Figure 3. SEM after 24 h of steel treatment.

In Figure 4, the evolution of the polarisation resistance (Rp) of the sample treated with B2_9 shows an increase in Rp until a value of about 500 Ohm cm^2 in 7 min. After that, the values of Rp remain constant because after 7 min, the coating completely covers the surface of steel, so stabilisation and saturation occurred.

As shown in Figure 5, SEM observations of the surface of coated sample (B2_9) show that the coating formed in this bath is cohesion leading to large flakes of ZP coating. When the concentration of nickel ions (Ni^{+2}) is little, the number of active centres on the surface is high and the process of crystal formation is much faster. So the coating was formed of inconsistent crystals. However, the coating of B2-1 has small cracks.

The coating does not cover the entire surface of the sample. The EDS analysis of the sample (B2_9) shows that the coating formed is more rich in phosphorus (14.5% P) and increasing in amount of zinc (27.2% Zn) with time than that obtained in the bath B2_1 (phosphorus (12.5% P) and zinc (18% Zn)).We noted by EDS analysis on bath B2 that the nickel sulphate acts as catalyst activator in the phosphating solution because nickel sulphate is the source for metal ions (Li & Sagüés, 2001; Palaniappa, Babu, & Balasubramanian, 2007).

Indeed, in the presence of a little nickel (B2), the layer growth increases until 7 min, and after that, it begins to decrease but (B2_9) becomes constant after 7 min.

3.1.3. Baths based on sodium nitrite, benzoate and citrate under the influence of zirconyl and copper (Table 6)

Four baths are used to evaluate the influence of copper amount and zirconyl nitrate amount. The pH values of the phosphating bath crystal (< 3) and observations on samples confirm pH values reported in the literature (Lorin, 1973). In the bath 3, we use zirconyl nitrate and copper oxide instead of nickel sulphate because zirconyl nitrate gives a good result in comparison of results of nickel sulphate (Adhikari et al., 2011). The zirconyl nitrate dissolves completely in that environment with a pH 2.5.

The evolution of the polarisation resistance of the sample was followed. Figure 6 shows that the growth kinetics is low during the first 3 min. During the next 7 min, the R_p increases to 6500 Ohm cm^2 for B3_1. The polarisation resistance of the samples increases with the decrease in the concentration of zirconyl.

SEM observations represented in Figure 7 show that the treatment with B3_1 promotes germination of the crystalline layer of zirconium. Crystals have sea anemone shape and cover almost the entire surface of the steel. We notice a change in crystal size according to the zirconyl content. If the zirconyl concentration increases, the crystal size decreases. So the coating is thinner and less compact in the presence of $ZrO(NO_3)_2$. H_2O (0.0024 g/l) in B3_3 in comparison with B3_1 ($ZrO(NO_3)_2.H_2O$ (0.0006 g/L)). EDS measurements show that B3-1 contains about 19.2% of Zn and 9.5% of P. However, for B3-3, the amount of zinc is 10.3% and 3.6% for P.

3.1.4. Baths based on hexametaphosphate and citrate ions under influence of phosphorus (Table 7)

To analyse the effect of the concentration of phosphorus (PO_4^{3-}) in the presence of Ni^{+2} on germination and growth of the phosphate layer formed on steel, we carried out the development of this coating under the same experimental conditions. The evolution of the polarisation resistance of phosphate coating for 10 min treatment of the sample in these baths is shown in Figure 8.

The curve shows that the phosphate layer begins to form after 4 min. Moreover, the growth kinetics of this layer is much lower compared to that observed previously in the baths B1 and B3 due to variation in composition compound. Too much of phosphoric acid not only delays the formation of the coating, but also leads to decrease in the polarisation resistance and finally leads to excessive metal loss. Polarisation may decrease when the concentration of phosphoric acid increases and the vapour activity increases, which essentially depends on the temperature.

SEM observations of the crystals obtained in the bath B4_5 showed that the crystals are much smaller than B4_1, and there are some small cracks in the coating layer. Although B4_1 is the best one in this group, poor phosphate layer is formed on steel (Figure 9). SEM observations show the formation of some small cracks on the surface of the sample. This report represents the limit of the acidity of the bath for the treatment of phosphate and this agrees with (Simescu, 2008). These observations made B4 coating less attractive.

According to EDS analysis, evolution of the polarisation resistance during treatment of the sample shows decrease in zinc, increase in Fe elements, while phosphorous and oxygen remain constant. The previous studies point out the importance of the proportion Zn^{+2}/PO_4^{-3} on the formation of ZP crystals (Ying et al., 1995). In our case, a ratio adjustment ZnO/H_3PO_4 has been implemented to improve germination and increase crystal size to make a total recovery of the surface.

The previous studies mentioned that when the ratio [ZnO/H_3PO_4] was from 0.3 to 0.4 (Simescu, 2008), the quality of coating increased. In fact, as the formation of the deposit is late, steel is exposed about sixty minutes to the acid attack (some samples), which causes the formation of a poor zinc deposit.

3.1.5. Choosing the best three baths of ZP

Under these conditions, the superposition of polarisation resistance curves obtained during treatment (Figure 2, 4 and 6) highlights the highest three values of polarisation resistance from each type of bath. The classification established for coating in this study is low quality 100 Ohm $cm^2 < Rp < 495$ Ohm cm^2, medium quality

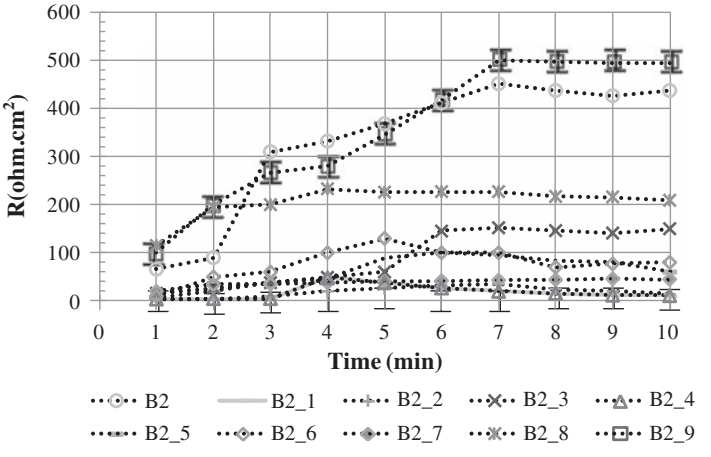

Figure 4. Values of polarisation resistance.

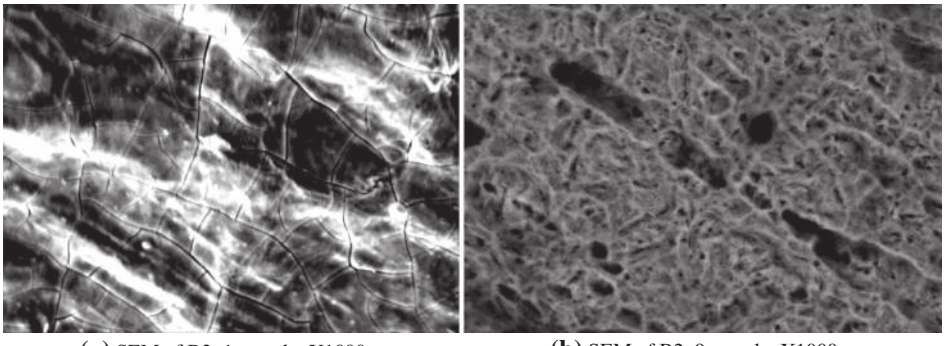

(a) SEM of B2_1 sample, X1000. **(b)** SEM of B2_9 sample, X1000.

Figure 5. Scanning electron microscope (SEM) after 24 h of steel treatment.

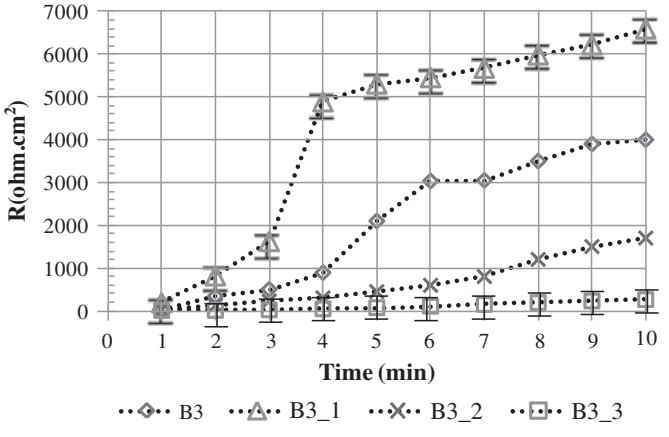

Figure 6. The values of polarisation resistance.

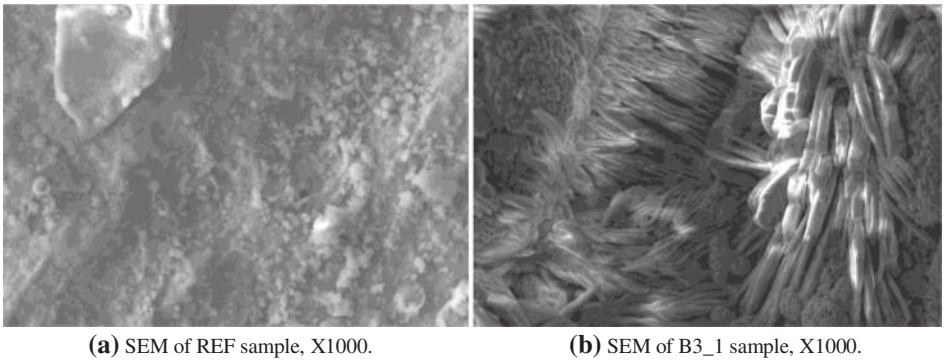

(a) SEM of REF sample, X1000. **(b)** SEM of B3_1 sample, X1000.

Figure 7. SEM after 24 h of steel treatment.

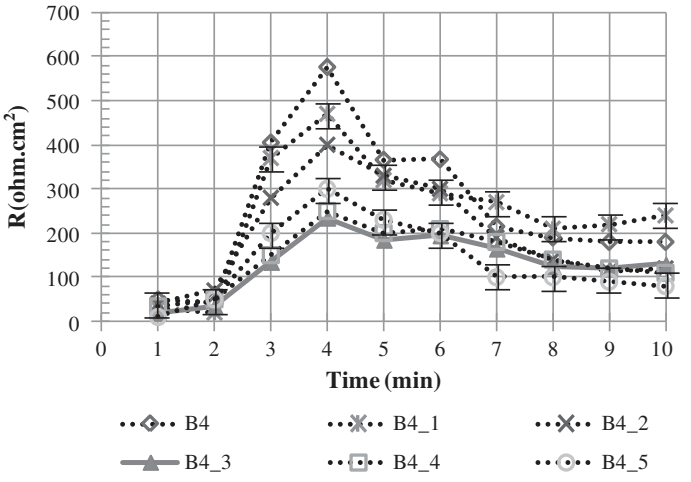

Figure 8. The values of polarisation resistance.

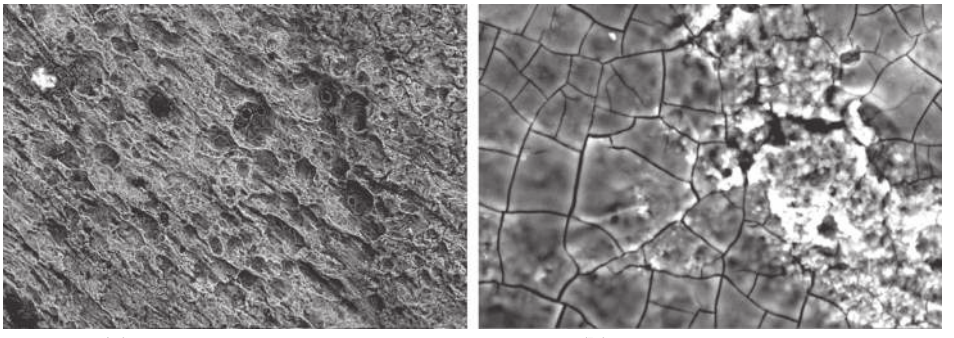

(a) SEM of B4_5 sample, X1000. **(b)** SEM of B4_1 sample, X1000.

Figure 9. SEM, after 24 h of steel treatment.

185 Ohm cm^2 < R*p* < 6591 Ohm cm^2 and high quality 240 Ohm cm^2 < R*p* < 9082 Ohm cm^2. These types were differentiated according to its quality by SEM, EDS modes, into high quality (B1-9), medium quality (B3-1) and low quality (B2-9) (Figure 10). In the three baths, we noticed the formation of a white precipitate at the bottom of the phosphating bath when the temperature exceeds 60 °C. Literature (Guenbour, Benbachir, & Kacemi, 1999; Lorin, 1973) shows that phosphatation treatment leads to the formation of two types of ZP. Firstly, hopeite Zn_3 (PO_4) $4H_2O$ and phosphophyllite ZnFe $(PO_4)2$ $4H_2O$ are formed for B2-9,B1-9. Secondly, hopeite, phosphophyllite and zirconia (ZrO_2) plates are formed for B3-1. Indeed, the baths used are not agitated. Under these conditions, the renewal of the solution in the steel is low (Psychoyos, 1990). Therefore, the formation of phosphophyllite is related to the presence of metal cations (Fe^{+2}) in the vicinity of the sample (Castagnola & Dutta, 2001; Frost, 2004). These two types of products (hopeite and phosphophyllite) are due to the acid attack of the sample, see Equations (1) and (2)).

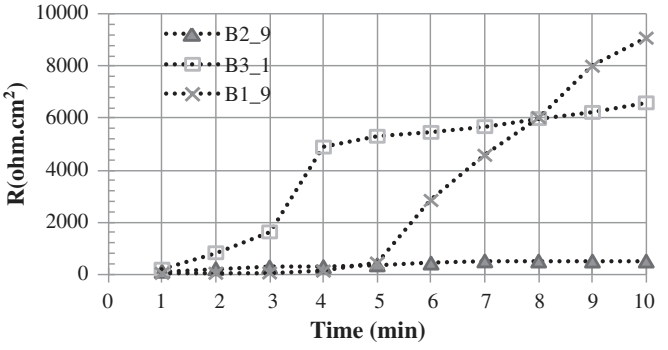

Figure 10. Values of polarisation resistance for the best baths of coating.

$$3Zn^{+2} + 2H_2PO_4^- + 4H_2O \rightarrow Zn_3(PO_4)_2.4H_2O + 4H^+ \quad (1)$$

$$2Zn^{+2} + Fe^{+2} + 2H_2PO_4^- + 4H_2O \rightarrow Zn_2Fe(PO_4)2.4H_2O + 4H^+ \quad (2)$$

3.2. Cathodic electrochemical treatment (CET) method

We used CET on steel with the selected three baths of high quality (B1-9), medium quality (B3-1) and low quality (B2-9).

3.2.1. Results of carbon steel immersed in synthetic solutions S1 after coating treatment

After applying coating, the potential of steel without coating increases due to the presence of oxides (Fe_3O_4 and Fe_2O_3) on the surface of steel.

The order of I_{corr} from high to weak: Ref steel > low quality > medium quality > high quality. Figure 11 shows a Nyquist plot of the impedance for three types of

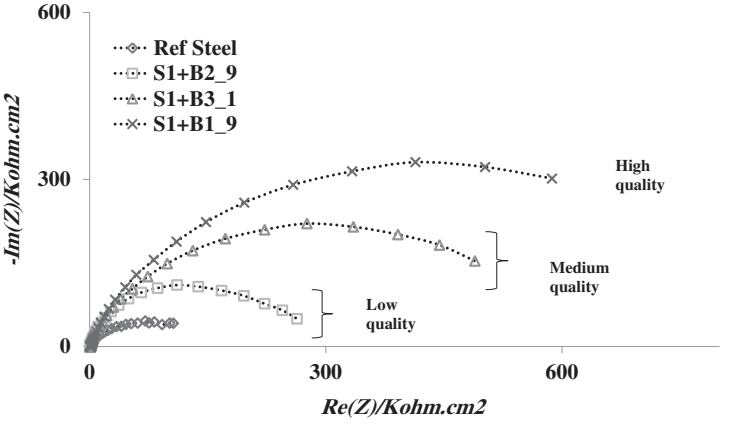

Figure 11. Nyquist plots for carbon steel with and without zinc phosphate treatment after 7 days in S1.

coating in fresh concrete pore solution S1. The electrochemical parameters (Rel: resistance of electrolyte, Rf: film resistance formed in alkaline solution, Rct: charge transfer resistance and Cf:A capacity film)are listed in Table 8 for steel after 7 days of immersion. The order of EIS quality of coating and E_{pit} from high to low: B1_9 > B3_1 > B2_9 > Ref steel according to the values of Rct.

The SEM observations show that the coating made from low quality which has cauliflower, Figure 12(b), is more prone to instability in alkaline solution compared to medium and high quality. Figure 12(c) clarifies the structure of medium quality which consists of a few small areas of hopeite characterised by plate- or flower-like crystals. It was found that the high quality of ZP coating is compact, well crystallised and covers completely the steel surface of shiny spots of seeds (Figure 12(d)) in the alkali solution S1: this figure gives evidence that the sample is almost composed of ZP.

3.2.2. Results of carbon steel immersed in synthetic solutions with chloride (S2) after coating treatment

According to ASTM standard C876–99 (ASTM Standard C876-99, 1999), after 7 days the rest potentials for S2 with high and medium quality shifted towards more positive values and are more homogeneous (−400 mV ± 100 mV).However, the rebar in S2 without coating shifted towards more negative. This indicates the beneficial role of quality of ZP (as a mean of protection against corrosion (formation of iron phosphate FePO4: protective layer)) in the presence of chloride, see Equation (3) and Figure 13. The rest potential for S2 with low quality is also shifted towards more positive value around −720 mV.

$$Zn_3PO_4(aq) + FeCl_3(aq) = 3\ ZnCl\ (aq) + FePO_4(s) \quad (3)$$

Table 8 and Figure 14 demonstrates the corrosion currents of rebars decrease with the increase in quality of ZP especially in the presence of chloride. After 7 days, the corrosion activity of the rebars in S2 with high-quality coating is negligible to weak because the average corrosion current value is equal to ((0.39 ± 0.05) μA/cm²). But S2 with medium quality shows a corrosion current (1 μA/cm²), indicating a limit corrosion activity of the rebars according to RILEM studies (Andrade & Alonso, 2004).

Figure 15 shows a Nyquist plot of the impedance of treated steel immersed in the fresh concrete pore solution S2. The chloride presence in S2 increases the resistance of ZP coating. This indicates the beneficial role of ZP coating in the presence of chloride. The electrical parameters are listed in (Table 8).

Table 8. Electrical parameters for treated and untreated carbon steel immersed in S1 and S2 solution obtained through fitting EIS data.

Bath number	S1				S2			
Sample	Ref steel	B2_9	B3_1	B1_9	Ref steel	B2_9	B3_1	B1_9
E_{corr} (mV/SCE)	−1162	−729	−419	−353	−220	−673	−393	−383
I_{corr} (μA/cm^2)	13.32	2.38	1.21	0.43	3.28	0.92	0.57	0.39
R_f(kΩ.cm^2)	–	1.07	1.20	8.00	–	0.22	0.46	1.29
R_{ct}(kΩ.cm^2)	9.5	26	66	97	106	263	489	587
C_{dl}(μF/cm^2)	70.01	67.6	29.6	9.6	44.8	1.81	1.06	0.24
E_{pit} (mV/SCE)	−482	−282	−266	−185	404	504	630	640

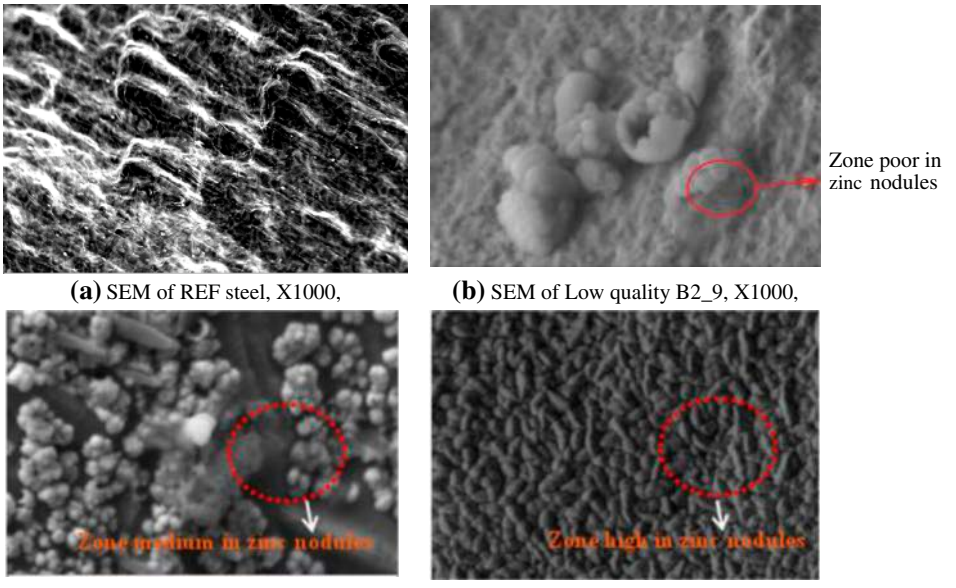

(a) SEM of REF steel, X1000, **(b)** SEM of Low quality B2_9, X1000,

(c) SEM of medium quality B3_1, X1000 **(d)** SEM of high qualityB1_9, X1000

Figure 12. SEM micrograph of carbon steel-coated surface after 7 days in S1.

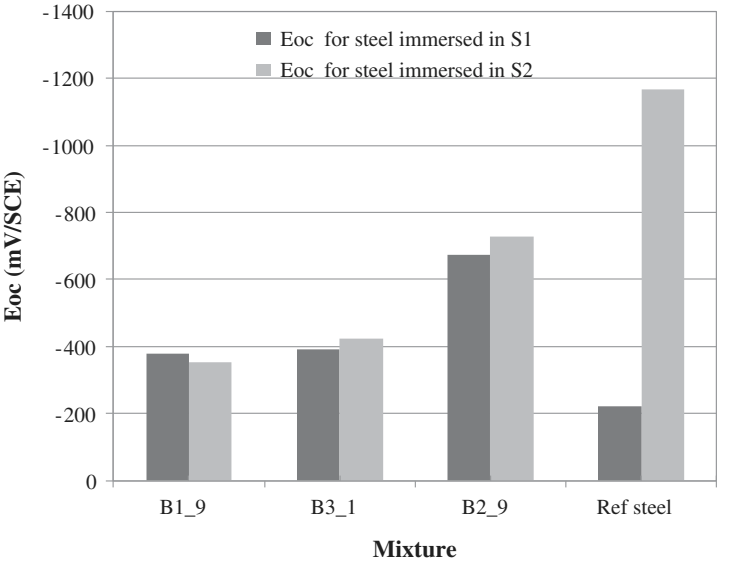

Figure 13. Corrosion potential for metal immersed in pore solution S1 and S2 after 7 days.

The effect of ZP coating in S2 can be noticed in the decreasing value of E_{pit} with the decrease in quality of ZP. E_{pit} for high quality had the same value of + 640 mV vs. SCE in S1 solutions and decreased to be −185 mV vs. SCE in S2, respectively. In these solutions, the E_{pit} had the value which is an indication that the steel treated with

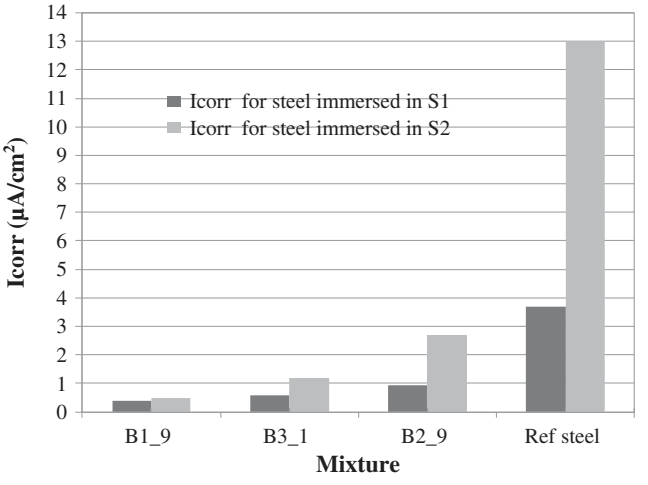

Figure 14. Corrosion currents for metal immersed in pore solution S1 & S2.

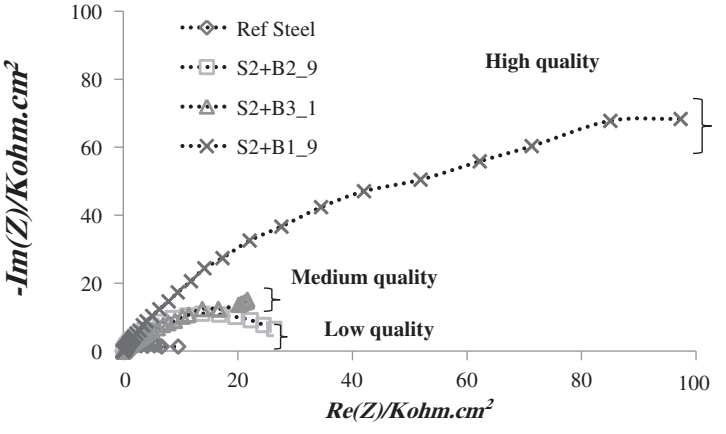

Figure 15. Nyquist plots for carbon steel with and without zinc phosphate treatment after 7 days in S2.

inhibitor (ZP) is able to resist pitting corrosion at these chloride levels Table 8. E_{pit} for Ref steel is −482 mV, this is an indication of the breakdown of the passive film of Ref steel (was not able to heal) in the presence of chloride ions. We use potentiostat to measure pitting corrosion using GC technique (General Corrosion).

Figure 16(a) and (b) shows the change in R_{ct} and passive film in case of S1 and S2. Basically, the passive film has a high resistivity for high, medium and low quality of ZP in pore solution S2 compared to the reference but S1 has more resistivity than S2 due to the presence of chloride.

SEM in this study reported that the low-quality film morphology of coral reefs formed in the presence of chlorides becomes thicker, but more porous and hydrated, losing its protective character. Because EDS analysis for low quality shows that, after 7 days of immersion, the coating composed of little quantity of P (phosphate element) and little of Zn Figure 18(a),(b) compared to that of high quality.

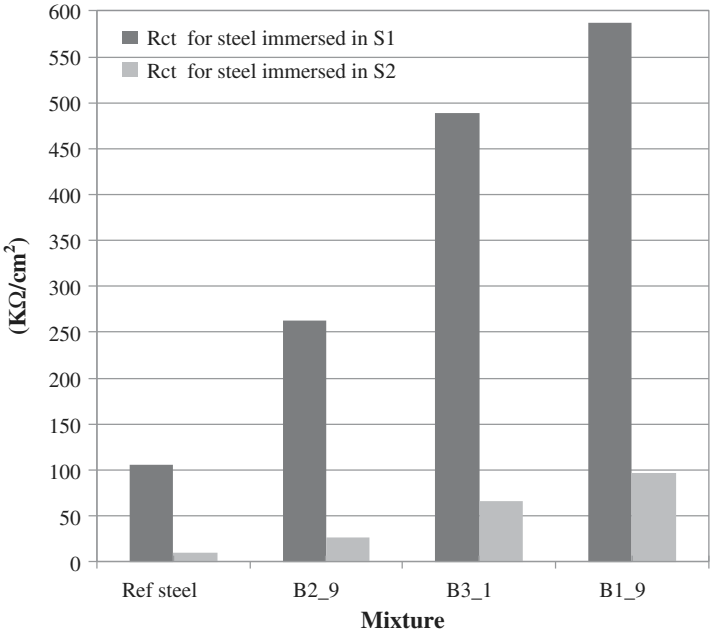

(a) Charge transfer resistance (Rct) in S1 and S2.

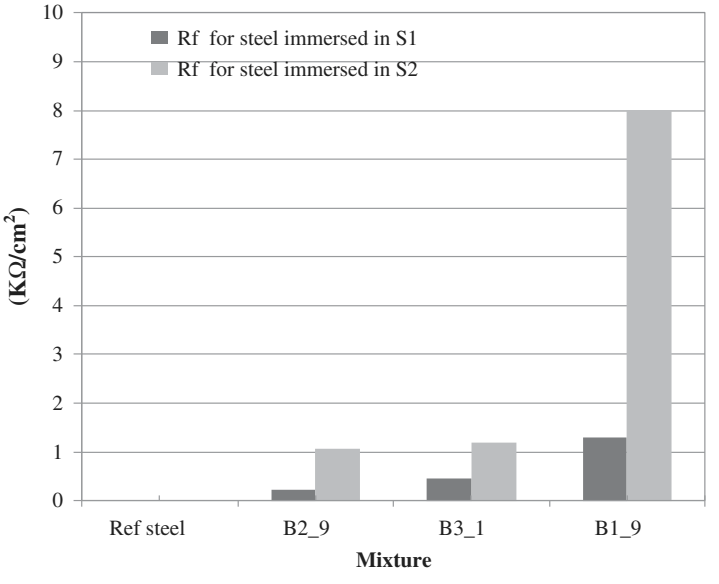

(b) Film resistance (Rf) in S1 and S2.

Figure 16. Charge transfer and film resistance for carbon steel in S1 and S2.

In case of medium quality, the presence of chlorides reports that the composition of the passive film morphology of ice is modified as reported in Figure 18(c),(d). This film was analysed using EDS and found to be hopeite $Zn_3\ (PO_4)_2 \bullet\ 4H_2O$ and phosphophyllite $Zn_2Fe\ (PO_4)_2 \bullet\ 4H_2O$. The presence of the phosphophyllite phase is related to the

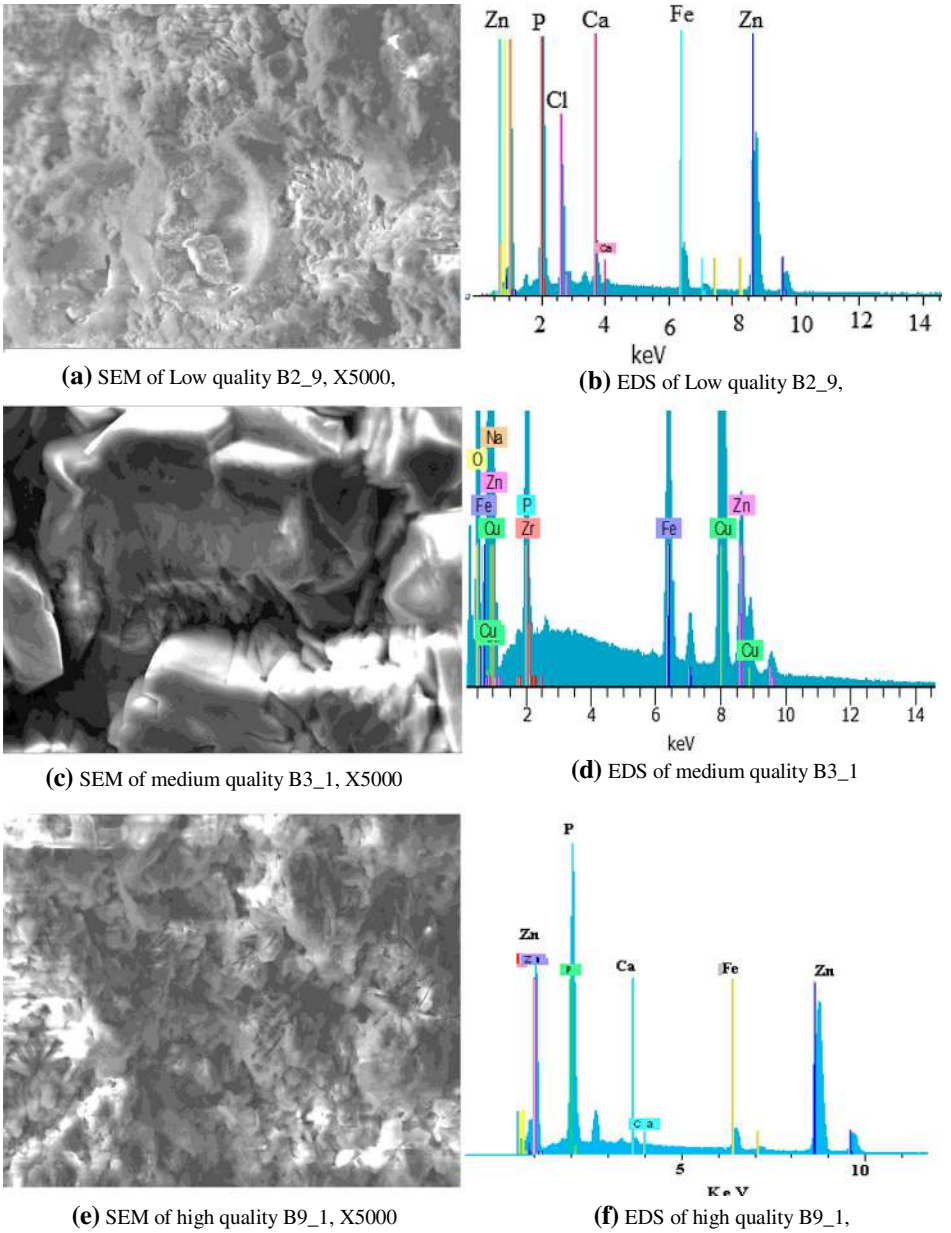

(a) SEM of Low quality B2_9, X5000,

(b) EDS of Low quality B2_9,

(c) SEM of medium quality B3_1, X5000

(d) EDS of medium quality B3_1

(e) SEM of high quality B9_1, X5000

(f) EDS of high quality B9_1,

Figure 17. SEM and EDS for carbon steel-coated surface after 7 days in S2.

Ref steel dissolution in the acid bath (pH = 2.2) during the phosphate treatment (Palaniappa et al., 2007) and the possible reactions (see Equations (1) and (2)) for the hopeite and phosphophyllite formations.

In the case of the high quality of ZP, the film morphology of fossils sites is similar to that observed in the absence of chloride ions (Figure 17(e),(f)). SEM and the EDS show the presence of calcium cations and hydroxyl anions in the cement pore solution

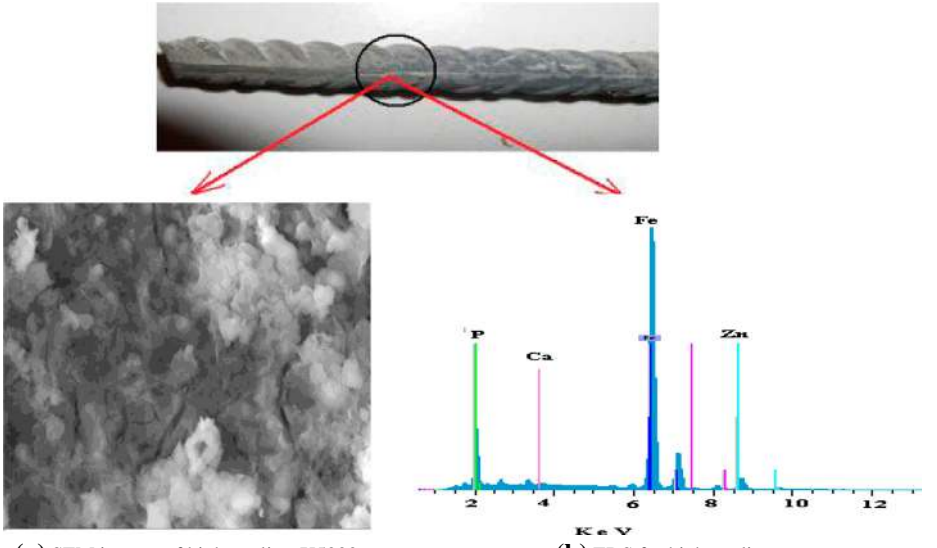

(a) SEM images of high quality, X5000. **(b)** EDS for high quality

Figure 18. SEM and EDS for carbon steel-coated surface after removal of mortar.

to form hydroxyapatite $Ca_{10}(PO_4)_6(OH)_2$. Thus, hydroxyapatite formation occurs even in the presence of chloride ions. The EDS shows that the coating composition for high quality is in 40 wt. % of zinc and 20 wt. % of phosphorus (Figure 17(e),(f)).

3.3. Corrosion behaviour of steel treated by ZP coating in OPC mortar

The SEM images of the high-quality sample show the formation of small hexagonal crystals at the phosphate coating/concrete interface (Figure 18(a)). Results of the EDS show that these crystals are composed of P, O and Ca (Figure 18(b)). Indeed, EDS confirms that the ZP coating protects the reinforcement and delays the initiation of its corrosion when embedded in mortar admixed with chlorides.

4. Conclusion

Three types of ZP were selected from the thirty baths and have been utilised in this study. These types were differentiated (according to its quality) using scanning electron microscopy (SEM) and energy dispersive spectroscopy (EDS) modes and classified into high quality (B1-9), medium quality (B3-1) and low quality (B2-9).

In this study, the ZP coating delays the time to depassivation, reduces the rate of corrosion in concrete and finally retards incipient action. Phosphate coatings are formed after immersing a steel substrate in a special ZP solution.

This study focused on the new development and achievement of the phosphate coating by CC. Thus, we have shown that it is possible to phosphating carbon steel by CC in the phosphating bath containing on the phosphoric acid, nitric acid, zinc, zirconium, copper and nickel ions.

New protective coatings have been developed by CET on reinforcing bars to prevent its corrosion in concrete. The coatings obtained using the phosphate processes are composed of two phases: hopeite and phosphophyllite.

Results showed that the increased weight of coating made by CC is consistent with the development of the polarisation resistance and corrosion potential of samples studied.

The effect of nickel ions on the structure of phosphate coating formed was showed: they give rise to a uniform, more dense coating, which composed of many small crystals of size. The EDS analysis showed that these coatings consist of zinc, iron, oxygen and phosphorus.

This experimental study has shown the effectiveness of some inhibitors: high, medium and low quality of ZP on concrete pore solution behaviour and reinforced concrete protection.

In alkaline solution with or without chloride, the phosphated mild steel sample is more resistant than mild steel alone. The metal of zinc, in the presence of calcium, forms a complex hydroxyzincate that is followed by the precipitation of calcium hydroxyzincate ($Ca(Zn(OH)_3)_2$. $2H_2O$) causing passivation of steel in concrete. Thus, a dense and protective layer is formed.

With a chloride ion solution, at very high concentrations exceeding the chloride threshold tolerated for the start of steel corrosion in alkaline media ($[Cl^-]/[OH^-] > 0.6$), the calcium hydroxyzincate film formed by this treatment contributes to the decrease in the aggressiveness of chloride and provides an effective protection against the corrosion of steel reinforcements.

Disclosure statement

No potential conflict of interest was reported by the authors.

References

Adhikari, S., Unocic, K. A., Zhai, Y., Frankel, G. S., Zimmerman, J., & Fristad, W. (2011). Hexafluorozirconic acid based surface pretreatments: Characterization and performance assessment. *Electrochimica Acta, 56*, 1912–1924.

Alonso, C., Andrade, C., Castellote, M., & Castro, P. (2000). Chloride threshold values to depassivate reinforcing bars embedded in a standardized OPC mortar. *Cement and Concrete Research, 30*, 1047–1055.

Andrade, C., Alonso, A., & Al. (2004). Test method for on-site corrosion rate measurement of steel reinforcement in concrete by means of the polarization resistance method. RILEM TC 154-EMC: Electrochemical Techniques for Measuring Metallic Corrosion – Recommendations, *Materials and Structures, 37*, 623–643.

Andreatta, F., Paussa, L., Lanzutti, A., Rosero Navarro, N. C., Aparicio, M., Castro, Y., Duran, A., Ondratschek, D., & Fedrizzi, L. (2011, September–October). Development and industrial scale-up of ZrO2 coatings and hybrid organic–inorganic coatings used as pre-treatments before painting aluminium alloys. *Progress in Organic Coatings, 72*, 3–14.

ASTM Standard C876-99. (1999). *Standard Test Method for Half-Cell Potentials of Uncoated Reinforcing Steel in Concrete*. West Conshohocken, PA: ASTM International. doi: 10.1520/C0876-91R99, Www.Astm.Org. (1999).

Burokas, V., Martušienė, A., & Bikulčius, G. (1998). The influence of hexametaphosphate on formation of zinc phosphate coatings for deep drawing of steel tubes. *Surface and Coatings Technology, 102*, 233–236.

Castagnola, M. J., & Dutta, P. K. (2001). Raman microprobe studies of dissolution of microporous faujasitic-like zincophosphate crystals. *Microporous and Mesoporous Materials, 42*, 235–243.

Frost, R. L. (2004). An infrared and Raman spectroscopic study of natural zinc phosphates. *Spectrochimica Acta Part A: Molecular and Biomolecular Spectroscopy, 60*, 1439–1445.

González, J. A., Ramírez, E., & Bautista, A. (1998). Protection of Steel Embedded in Chloride-Containing Concrete by means of Inhibitors. *Cement Concrete Research, 28*, 577–589.

Guenbour, A., Benbachir, A., & Kacemi, A. (1999). Evaluation of the corrosion performance of zinc-phosphate-painted carbon steel. *Surface and Coatings Technology, 113*, 36–43.

Hurley, M. F. (2007). *Corrosion initiation and propagation behaviour of corrosion resistant concrete reinforcing materials* (PhD thesis). University of Virginia, USA.

Kouisni, L., Azzi, M., Zertoubi, M., Dalard, F., & Maximovitch, S. (2004). Phosphate coatings on magnesium alloy AM60 part 1: Study of the formation and the growth of zinc phosphat. *Surface & Coatings Technology, 185*, 58–67.

Li, L., & Sagüés, A. A. (2001). Chloride corrosion threshold of reinforcing steel in alkaline solutions—open-circuit immersion tests. *Corrosion, 57*, 19–28.

Lorin, G. (1973). *La phosphatation des métaux*. Paris: Editions Eyrolles, p. 229.

Manna, M. (2009). Characterisation of phosphate coatings obtained using nitric acid free phosphate solution on three steel substrates: An option to simulate TMT rebars surfaces. *Surface & Coatings Technology, 203*, 1913–1918.

Nedal, Mohamed. (2009). *Comparative Study of the Corrosion Behaviour of Conventional Carbon Steel and Corrosion Resistant Reinforcing Bars*. A Thesis Submitted for the Degree of Master of Science University of Saskatchewan. August 2009.

Palaniappa, M., Babu, G., & Balasubramanian, K. (2007). Electroless nickel–phosphorus plating on graphite powder. *Materials Science and Engineering A, 471*, 165–168.

Psychoyos, N. (1990). *Traitements de preconversion des tolesrevetues de zinc: Caracterisation physico-chimique des couches creees* (Thesis), Lyon-1 Univ., France.

Simescu, F. L. (2008). *Elaboration des revêtements de phosphates de zinc sur armature à béton. Etude de leur comportement à la corrosion en milieu neutre et alcalin* (PhD thesis). INSA de Lyon – DOC'INSA – CITHER, France.

Simescu, F., & Idrissi, H. (2009). Corrosion behaviour in alkaline medium of zinc phosphate coated steel obtained by cathodic electrochemical treatment. *Corrosion Science, 51*, 833–840.

Veleva, L., Alpuche-Aviles, M. A., Graves-Brook, M. K., & Wipf, D. O. (2005). Voltammetry and surface analysis of AISI 316 stainless steel in chloride-containing simulated concrete pore environment. *Journal of Electroanalytical Chemistry, 578*, 45–53.

Ying, J. F., Flinn, B. J., Zhou, M. Y., Wong, P. C., Mitchell, K. A. R & Fostert, T. (1995, September–December). Optimization of zinc phosphate coating on 7075-T6 aluminum alloy. *Progress in Surface Science, 50*, 259–267.

Zeng, R., Lan, Z., Kong, L., Huang, Y., & Cui, H. (2011, 25 February). Characterization of calcium-modified zinc phosphate conversion coatings and their influences on corrosion resistance of AZ31 alloy. *Surface and Coatings Technology, 205*, 3347–3355.

Zimmermann, D., Mun˜oz, A. G., & Schultze, J. W. (2005). Formation of Zn–Ni alloys in the phosphating of Zn layers. *Surface & Coatings Technology, 197*, 260–269.